REVISTA FLORESTA Engenharia Florestal
ISSN 1982-4688
Edição 55
Universidade Federal do Paraná
Setor de Ciências Agrárias

SENSITIVITY OF C-VV AND C-VH POLARIZATIONS FOR EDGE EXTRACTION BY MATHEMATICAL MORPHOLOGY IN A DEFORESTATION

Juarez Antônio da Silva Júnior[1*], Ubiratan Joaquim da Silva Júnior[2], Fabio Vinicius Marley Santos Lima[3], Admilson da Penha Pacheco[4]

[1*]Universidade Federal de Pernambuco (UFPE), Departamento de Engenharia Cartográfica - Recife, Pernambuco, Brasil – juarez.silvajunior@ufpe.br
[2]Universidade Federal de Pernambuco (UFPE), Departamento de Engenharia Cartográfica - Recife, Pernambuco, Brasil – ubiratan.joaquim@ufpe.br
[3]Universidade Federal do Rio Grande do Norte (UFRN), Programa de Pós-Graduação em Ciências Climáticas - Natal, Rio Grande do Norte, Brasil – fabio.vinicius@ufpe.br
[4]Universidade Federal de Pernambuco (UFPE), Departamento de Engenharia Cartográfica - Recife, Pernambuco, Brasil – admilson.pacheco@ufpe.br

Received for publication: 15/09/2022 – Accepted for publication: 03/02/2025

Resumo

Sensibilidade das polarizações C-VV e C-VH para extração de borda por Morfologia Matemática em um desmatamento. As florestas tropicais, a exemplo da Amazônia, representam importantes reservas de biodiversidade. Entretanto, processos como o desmatamento tem proporcionado a redução da cobertura vegetal. O objetivo deste estudo foi realizar a extração de bordas, num polígono de desmatamento contido numa cena do Satélite Sentinel 1, utilizando a técnica de Morfologia Matemática, na floresta Amazônica, no estado do Mato Grosso, Brasil. A metodologia foi desenvolvida para obtenção das bordas externa, interna e gradiente da feição de corte raso, por meio da implementação de operações aritméticas de dilatação e erosão na imagem de radar nas polarizações VH e VV. Foram utilizadas imagens do satélite Sentinel 2 na mesma data de aquisição das imagens SAR comparando espacialmente as bordas obtidas pelas polarizações VH e VV. Como resultado, a borda gradiente apresentou um delineamento com um ruído e espaçamento menor em relação as bordas externas e internas. Áreas com mudanças texturais abruptas exibiram bordas bem definidas e isentas de ruídos para as diferentes polarizações. Por outro lado, em locais com maior variabilidade de sinal, como regiões agrícolas, foram observadas bordas caracterizadas por segmentos dispersos e alta distribuição de ruído. Ainda assim, as bordas geradas pelas polarizações não apresentaram diferenças significativas entre si. Contudo, as bordas obtidas a partir da polarização VH destacaram-se por apresentar menor diferença e maior (R^2) em relação ao produto de referência. Isso sugere que a extração de bordas com base em polarizações cruzadas pode ser uma abordagem precisa para análises de perturbações em florestas tropicais, como no monitoramento do desmatamento.
Palavras-chave: Morfologia Matemática, Amazônia, SAR, Sentinel-1.

Abstract

Tropical forests, like the Amazon, represent important reserves of biodiversity. However, processes such as deforestation have led to a reduction in vegetation cover. The objective of this study was to perform the extraction of edges, in a polygon of deforestation contained in a scene of the Sentinel Satellite 1, using the technique of Mathematical Morphology, in the Amazon rainforest, in the state of Mato Grosso, Brazil. The methodology was developed to obtain the external, internal and gradient edges of the shallow cut feature, by implementing arithmetic operations of dilation and erosion in the radar image in the VH and VV polarizations. Images from the Sentinel 2 satellite were used on the same acquisition date as the SAR images, spatially comparing the edges obtained by the VH and VV polarizations. As a result, the gradient border presented an outline with a smaller noise and spacing in relation to the external and internal borders. Areas where there were abrupt textural changes presented well-defined edges and without the presence of noise for the polarizations. On the other hand, in locations with greater signal variability, such as agricultural regions, edges characterized by dispersed segments and high noise distribution were observed. Even so, the edges generated by the polarizations did not present significant differences between them. However, the edges obtained from the VH polarization stood out for presenting a smaller difference and higher (R^2) in relation to the reference product. This suggests that edge extraction based on cross-polarizations can be an accurate approach for analyzing disturbances in tropical forests, such as in deforestation monitoring.
Keywords: Mathematical Morphology, Amazon, SAR, Sentinel-1.

INTRODUCTION

Forests cover approximately 30% of the Earth's surface and are crucial for regulating climate, maintaining biodiversity, and supporting ecosystems and human communities. However, deforestation and forest loss pose severe global threats to environmental sustainability and ecosystem balance (Drüke & Thonicke, 2023). The main

drivers of deforestation include agricultural expansion, livestock farming, urbanization, and forest fires (Silva Júnior *et al.*, 2020). These activities lead to habitat fragmentation, biodiversity loss, and increased greenhouse gas emissions, exacerbating climate change (Yang *et al.*, 2025). Addressing these challenges requires balancing natural resource use with conservation strategies. The destruction of forests alters landscapes and has severe environmental consequences, including carbon emissions, habitat destruction, and the reduction of essential ecosystem services (Dias *et al.*, 2025). The loss of forests threatens the livelihoods of millions and contributes to about 10% of global CO_2 emissions. Monitoring deforestation is essential for protecting ecosystems, particularly in the Brazilian Amazon, one of the most endangered regions (Silva *et al.*, 2021). Remote sensing plays a key role by providing periodic and precise data on deforestation, even in areas with cloud cover or limited accessibility. Synthetic Aperture Radar (SAR) enables nighttime and all-weather monitoring, enhancing global forest conservation efforts.

Synthetic Aperture Radar (SAR) sensors are highly effective for monitoring tropical forests, as they can acquire data regardless of cloud cover. This is particularly important in tropical regions, where persistent cloudiness limits the effectiveness of optical sensors, which rely on clear weather conditions. SAR technology ensures continuous data collection, enhancing the reliability of environmental analyses (Carreiras *et al.*, 2017). Its ability to operate in all weather conditions makes it invaluable for long-term ecological studies and real-time early warning systems, both of which are crucial for conservation efforts. The frequent presence of clouds in biodiversity-rich tropical and monsoon forests significantly reduces usable optical observations. However, SAR, which operates in the microwave spectrum, is minimally affected by atmospheric conditions, making it a key tool for forest monitoring (Reiche *et al.*, 2018). SAR data are often integrated with optical imagery for land cover classification and deforestation tracking (Arévalo *et al.*, 2020; Zhang *et al.*, 2021; McGregor *et al.*, 2024). ALOS-PALSAR data have demonstrated the effectiveness of L-band SAR in mapping tropical forests. Additionally, SAR sensors such as Radarsat, Sentinel-1, and ALOS-PALSAR utilize backscatter mechanisms to estimate biomass, soil moisture, and vegetation density, providing valuable insights into forest structure (Bouvet *et al.*, 2018; Ballère *et al.*, 2021).

Among the approaches that use Sentinel-1 backscatter data to detect deforestation, the use of Sentinel-1 time series with a stream of single images or a stream of small image clusters for feature edge detection and extraction stands out. Slagter *et al.* (2024) presented automated remote sensing-based methods to monitor road development in tropical forests between 2019 and 2022 for the entire Congo Basin forest, using deep learning techniques applied to Sentinel-1 and -2 images for accurate and timely road detections. McGregor, Connette, and Gray (2024) created a multi-source NRT monitoring algorithm by combining Sentinel-2 and Sentinel-1 data in northern Myanmar to monitor areas with contrasting forest types. Guisao-Betancur, Déniz, and Marulanda-Tobón (2024) conducted a literature review highlighting the potential observed in SAR data for the development of forest mapping and monitoring tools that can also be used for related applications such as agriculture or land use mapping. Bouvet *et al.* (2018) used the emerging and disappearing radar shadow effects due to the recording of tall trees to detect the edges of deforested areas. Ballère *et al.* (2021) developed a national-scale forest loss warning system for French Guiana based on the method developed by Bouvet *et al.* (2018) using Sentinel-1 SAR data.

Edge detection is a computational tool commonly used to obtain information on linear features on the Earth's surface, becoming essential in cartographic representation and description of territorial form, rivers, roads, among other features. Studies developed by Fonseca, Tavares Jr. and Candeias (2020) show that the automatic extraction of linear features from edge detection techniques emerges as a possibility for mapping degraded areas, such as incidences of deforestation and forest fires, allowing the interpretation of lineaments and recognition of patterns of use and coverage of forested areas in orbital images. The method aims to automatically transform linear features contained in images or geophysical data into a vector segment, accelerating the extraction process and reducing the subjectivity inherent in the manual method. According to Silva *et al.* (2021), the state of Mato Grosso, especially the Amazon/Cerrado transition region, deserves special attention in terms of monitoring the dynamics of land use and coverage, as it constitutes a front of agricultural expansion into the interior of the Brazilian Amazon.

Techniques such as edge extraction, which allow obtaining information on land cover automatically, reducing the subjectivity of manual methods, become tools that ensure accuracy and practicality, expanding the monitoring capacity of deforested areas. In this context, the objectives of this article are: i) To analyze the sensitivity of VV and VH polarizations in the C band for edge extraction by the Mathematical Morphology (MM) method, using a radar image from the Sentinel-1 satellite in a clear-cut area in the municipality of Alto Boa Vista - MT, located in the Brazilian Legal Amazon. ii) To evaluate the performance of the edge extraction method for each of the polarizations through visual analysis in comparison with multispectral data from the passive MSI sensor on board the Sentinel-2 satellite. iii) To identify and map deforestation points throughout the scene.

REVISTA FLORESTA Engenharia Florestal
ISSN 1982-4688
Edição 55
Universidade Federal do Paraná
Setor de Ciências Agrárias

MATERIAL AND METHODS

Study Area

The Amazon Biome is formed by nine countries in South America, but 69% of this extension belongs to Brazil, covering the states of Pará, Amazonas, Maranhão, Goiás, Mato Grosso, Acre, Amapá, Rondônia and Roraima, within a total area of 4,871,000 (km²). The state of Mato Grosso has an area of approximately 903 thousand (km²), of which 54% is occupied by the Amazon biome in the northern portion, 40% by the Cerrado in the central portion and 6% by the Pantanal in the southern portion (IBGE, 2004). The study area is formed by a polygon between the coordinates: 11°50'33.64"S, 52° 9'43.43"W and 11°44'51.95"S, 52° 3'1.17"W, in the extension of the Legal Amazon (Figure 1).

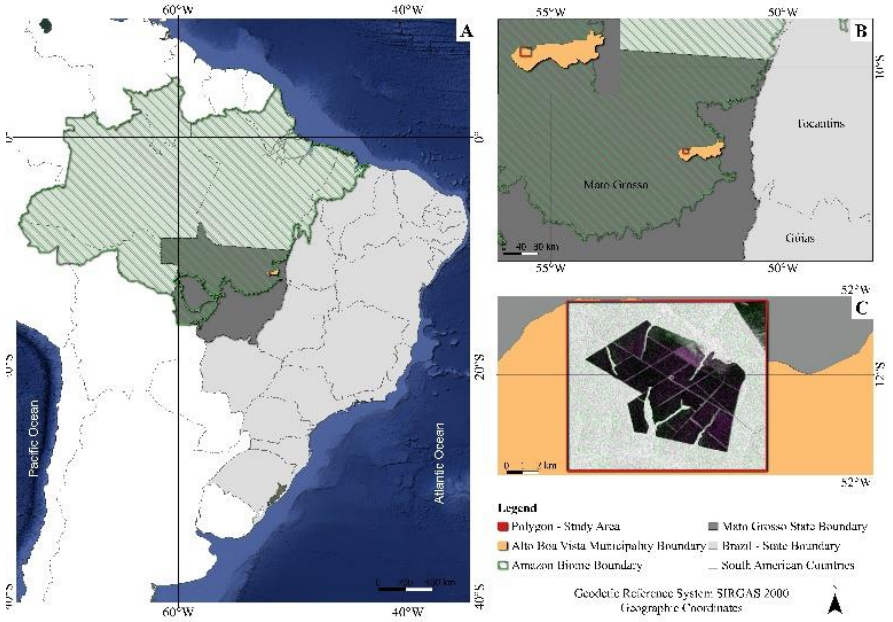

Figure 1. Study Area. (A) Amazon Biome. (B) Study area located in the State of Mato Grosso, Brazil. (C) Representation of the deforestation polygon, in a scene from the Sentinel 1 radar sensor.

Figura 1. Área de Estudo. (A) Bioma Amazônia. (B) Área de estudo inserida no Estado do Mato Grosso, Brasil. (C) Representação do polígono de desmatamento, numa cena do sensor radar Sentinel 1.

For the methodological development, an image from the Sentinel-1 radar sensor, captured on 09/08/2022, with an incidence angle of approximately 40°, was used. This image was obtained free of charge through the Copernicus portal, maintained by the European Space Agency (ESA), available at the link (https://scihub.copernicus.eu). Sentinel-1 consists of two identical satellites, 1A (S1A), launched in 2014, and 1B (S1B), launched in 2016. When both were operational, the repetition cycle was 6 days. The scene used in this study has processing level 1A and was acquired in Single Look Complex (SLC) and Ground Range Detected (GRD) formats. These SAR data are georeferenced based on satellite orbit and attitude information, presented in zero-doppler oblique ranging geometry, analyzed and projected to the ground range using an Earth ellipsoid model. In Interferometric Wide Swath mode, S1A provides data in VH (vertical-horizontal) cross-polarization and VV (vertical-vertical) co-polarization, covering a 250 km swath with a spatial resolution of 10 meters (ESA, 2021).

In this paper, the scene was processed in the SNAP Sentinel-1 Toolbox software using the following steps: Thermal noise removal, Radiometric calibration, Lee filter, Terrain correction using SRTM 30. The final terrain corrected values are converted to decibels via log scale (10*log10(x)). For spatial comparison of the results, a scene from the MSI multispectral sensor, on board the Sentinel-2 satellite, recorded on 09/10/2022, was used. In this study, only bands with a spatial resolution of 10 meters were considered. A threshold at σ0 was applied to classify the scene into the categories "forest" and "non-forest", using as a basis a deforestation mask obtained from the reference map of land use and occupation of the Amazon Deforestation Estimation Program (PRODES). This approach allowed minimizing ambiguities associated with the characteristics of the land cover elements, resulting in the extraction of a sample set of backscatter pixels for the "forest" and "non-forest" classes. From this, the average backscatter value (mpol) was calculated for each class in both polarizations.

Separability Analysis (M)

The Separability Test (M) was performed to quantify the distinction between forest and non-forest classes and determine a fixed threshold value (Pereira *et al.* 2016). The M index evaluates the signal-to-noise ratio, considering the absolute difference between the class means (signal) and the sum of the standard deviations (noise). This index, which ranges from 0 to 2, indicates high separability when M > 1 and low separability when M < 1 (Kaufman; Remer, 1994). The degree of thresholding is adjusted for each scene due to variations in environmental conditions and the acquisition system. In the study, the M index was also used to validate sample separability and evaluate the effectiveness of each polarization in discriminating between deforested and non-deforested areas (Libonati *et al.* 2015).

Hypothesis test for thresholding

The values of m_{VHnf} and $m_{VVnf}$for the non-forest class were used as thresholding criteria through the following hypothesis test: if the pixel is greater than the mean (m) it receives the value 1 (presence) or if the pixel is smaller than the mean it receives the value 0 (non-presence), based on the methodology developed by Pietro (2020). Equations 3 and 4 describe the hypotheses used in the test:

$$VH: 1\ se\ f(x,y) > m_{VHnf}\ e\ 0\ se\ f(x,y) < m_{VHf,} \quad (3)$$

$$VV: 1\ se\ f(x,y) > m_{VVnf}\ e\ 0\ se\ f(x,y) < m_{VHf}, \quad (4)$$

Where, f(x,y) represents the image, m_{VHnf} and m_{VVnf}represent the average of the values of the set of pixels in their respective polarizations of the forest and non-forest classes. In this way, an image f(x,y) was obtained for each polarization. After the hypothesis test, the edges of the deforested perimeter were extracted using the Mathematical Morphology method.

Mathematical Morphology

There are several methods for applying edge detection, one of the most frequently used techniques being directional filters. However, Mathematical Morphology has been increasingly used in research, especially in the field of geosciences (Jin *et al.* 2021). The basic principle of Mathematical Morphology consists of extracting information regarding the geometry and topology of an image f, using another defined set, called the structuring element (B) of dilation δB(f) or erosion εB(f) (Candeias; Moura; Nascimento, 2013). The equations that define the external, internal and gradient edges are presented below. Equation 5 defines the external edge feature by mathematical morphology:

$$f1 = \delta B(f) - f \quad (5)$$

Then we have Equation 6, defining the internal edge feature by mathematical morphology and Equation 7 the gradient:

$$f2 = f - \varepsilon B(f) \quad (6)$$

$$f3 = \delta B(f) - \varepsilon B(f) \therefore f3 = f1 + f2 \quad (7)$$

Each of the three edges has a result in the analysis of each feature.

Validation

To validate the edges obtained by SAR, a scene from the MSI sensor with bands 4 (red), 5 (Red Edge 1) and 6 (Red Edge 2) was used to extract deforested areas using the Reed-Xiaoli Detector (RXD) algorithm. This algorithm identifies spectrally distinct targets in binary classes, without the need for prior information. RXD distinguishes anomalous changes, such as deforested areas, from generalized variations, such as seasonal effects, using a covariance matrix to calculate the Mahalanobis distance between a pixel and the average of the pixels around it. The anomalous change (MA) score is then calculated by the algorithm following equation 8.

$$\mathrm{MA}(x) = (\mathrm{x}' - \mu)^{\mathrm{T}} \mathrm{C}^{-1} (\mathrm{x}' - \mu) \quad (8)$$

Where x is any given pixel, x′ is a vector formed by the values of the image bands of pixel x, μ is a vector composed of the mean value of the background pixels (e.g., stable areas) in each image band, and C is the covariance matrix of the image bands.

In a complementary manner, a graphical analysis using a Simple Linear Regression Model was performed to explore the relationship between the edges obtained by MM and the linear data of the reference product. The coefficient of determination (R^2) was used as a statistical metric to evaluate the quality of the fit and the correlation between the variables, indicating the model's ability to explain the variability of the observed data. In summary, the proportion of pixels of the edges obtained by MM in the VH and VV polarizations was compared to the proportion of cells detected by the reference data. R^2 served as a precision criterion, as described by Giglio *et al.* (2018).

RESULTS

Separability analysis between deforested and non-deforested areas

Table 1 describes the values of the Separability Index (M) and average backscattering values for the "forest" and "non-forest" classes in decibels (dB), obtained through processing.

Table 1. Values of the Separability Index (M) and mean values of backscattering for "forest" m_{polf} and "non-forest" $m_{polnf.}$

Table 1. Valores do Índice de Separabilidade (M) e valores médios de retroespalhamento para classe "floresta" m_{polf} e "não floresta" $mpol_{nf}$.

Polarization	M Separability	m_{polf} (dB)	m_{polnf} (dB)
VH	1,8	-12	-20
VV	1,7	-9	-14

Source: Authors, 2025.

High separability values (M > 1) are observed in both polarizations, with no significant variations between them. The average backscattering values (dB) in the forest and non-forest classes show greater intensity for the VV polarization. This result is in line with the typical behavior of direct and cross-polarizations in the C band, as described by Hansen, Mitchard and King (2020). In this band, backscatter in VH is predominantly caused by volumetric scattering from leaves and small branches, reducing when the canopy is lost due to deforestation. In VV, backscatter is more complex, as it reflects both canopy volume and double bounce scattering. In clear-cut areas, it is common to observe a reduction in backscatter in both polarizations, which may appear as suddenly darker patterns in SAR images compared to the surrounding intact forest.

Edge detection using Mathematical Morphology is a fundamental step in any image analysis system. Thus, it is essential to build a representative set of visual features that are directly related to and characterize the content of satellite images. In this context, figures 2 to 5 present a set of visual features used for the analysis of edges generated by MM in VV and VH polarizations.

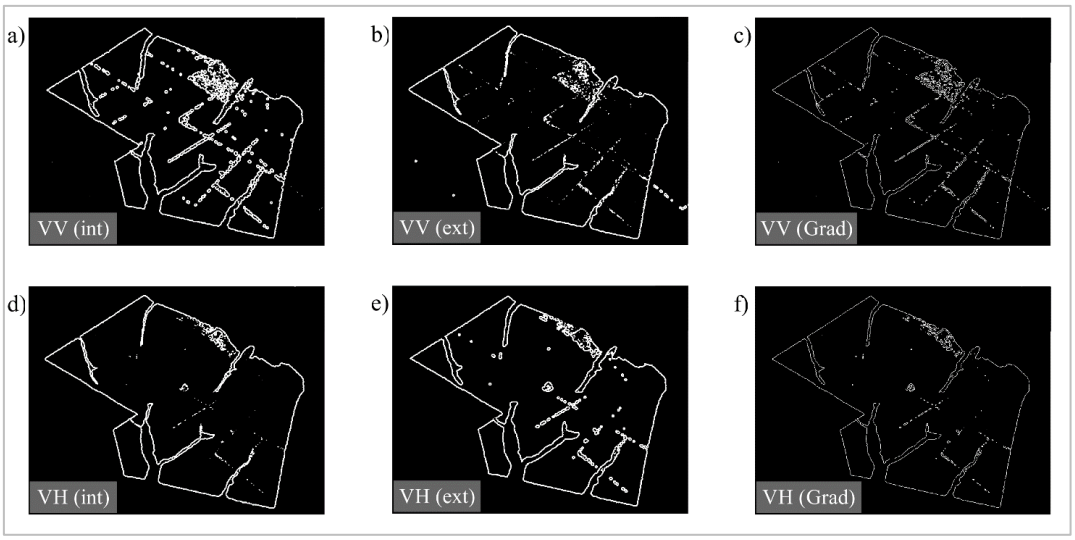

Figure 2. Spatial distribution of the internal, external edge and gradient in the VH and VV polarizations.
Figura 2. Distribuição espacial da borda interna, externa e gradiente nas polarizações VH e VV.

Using an RGB VV/VH/VV composition, Figure 3 illustrates the edges generated by abrupt changes in signal intensity, highlighting a noise-free delineation in the region where an abrupt transition occurred between the "forest" and "non-forest" classes. Figure 4 shows the edges generated in a sector where agricultural activity predominates.

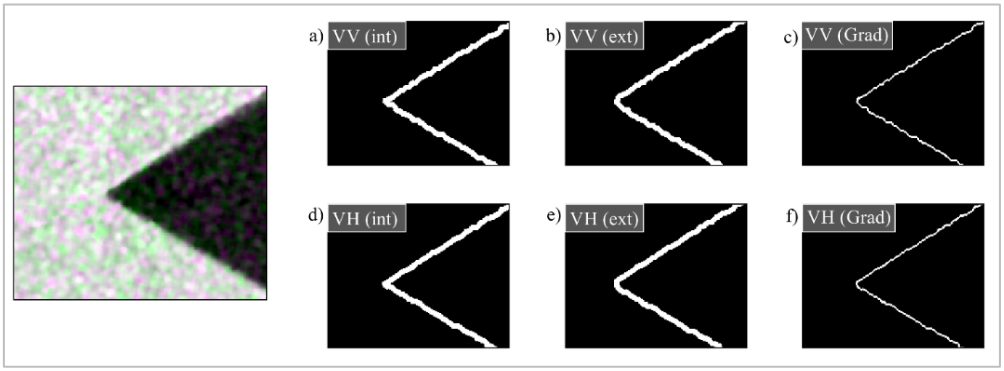

Figure 3. Edges generated by MM in the VH and VV polarizations in a clear cut area with an abrupt pattern.
Figura 3. Bordas geradas por MM nas polarizações VH e VV numa área de corte raso com padrão abrupto.

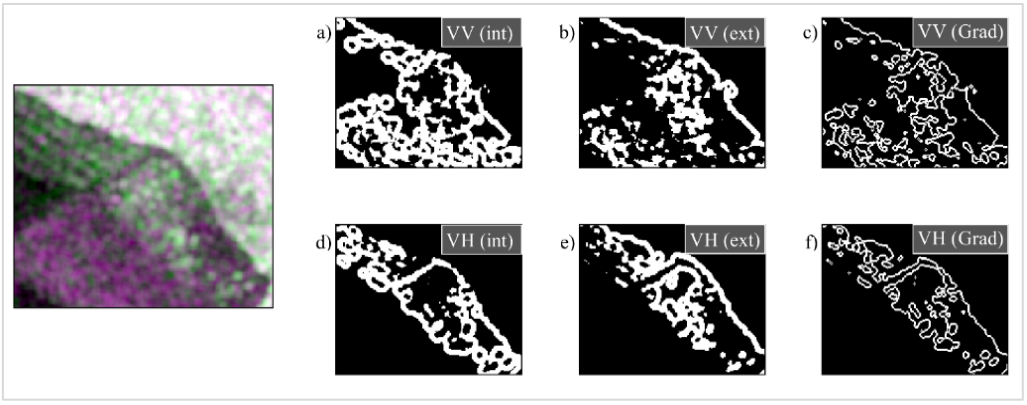

Figura 4. Edges generated in an agricultural part in the area of deforestation.
Figure 4. Bordas geradas numa parte agrícola na área de desmatamento.

In Figure 5, it is possible to observe, in the RGB VV/VH/VV composition, a mosaic of color patterns that indicate a large variability in backscattering in this area, which may have generated a significant noise distribution at the edges produced in both polarizations.

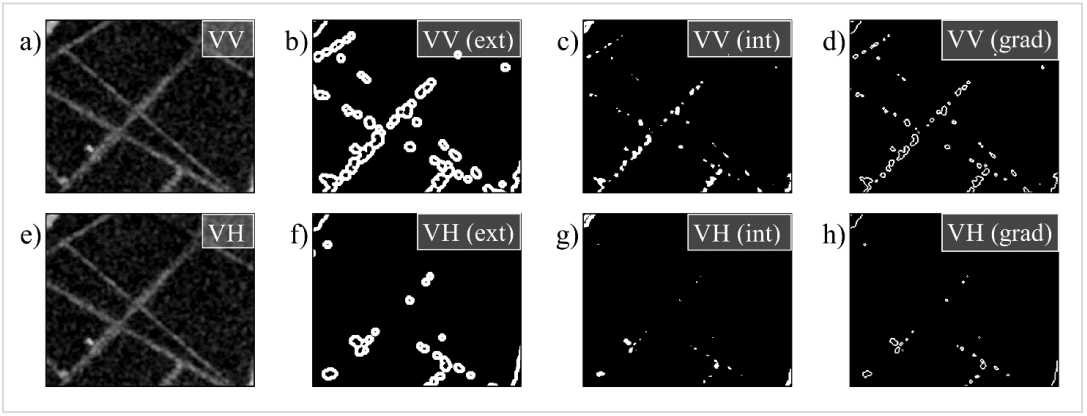

Figure 5. Lineament of deforestation included in the deforestation class.
Figura 5. Lineamento de desmatamento inseridas na classe de desmatamento.

According to Hansen, Mitchard, and King (2020), land cover types such as these can produce varying backscatter values, extending into the range of forest signatures, especially at shorter wavelengths such as the C and X bands. These signal types are less sensitive to forest structure, since the radar interacts mainly with the canopy. The presence of these gaps is expected, since agricultural areas and dry or wet soils have high sensitivity to signal return, especially in the VV polarization. However, the edges generated in the VH polarization show

REVISTA FLORESTA Engenharia Florestal
ISSN 1982-4688
Edição 55
Universidade Federal do Paraná
Setor de Ciências Agrárias

less noise visually. Figure 6 shows the edges generated on the deforestation lines in the study area, for each polarization separately.

Like the external edge, the gradient presented hollow, circular polygon segments without defined linear characteristics. The internal edge, on the other hand, exhibited compact and punctual features, dispersed among themselves. In general, the thresholding technique was unable to minimize the failures caused by the different soil features and deforestation lines in the study area, which resulted in a significant residual in relation to the reference data, as shown quantitatively in Table 2 and Figure 6.

Spatial comparison with the MSI sensor

Table 2 shows in spatial terms the areas obtained by the edges (km²) were compared with the Sentinel-2 data.

Table 2. Areas obtained by edges (Km²) compared to Sentinel 2 data.
Tabela 2. Áreas obtidas pelas bordas (Km²) comparadas com dados do Sentinel 2.

Edge	VV	VH	Discrepancy VV	Discrepancy VH
Internal edge	36,03	38,56	7,27	4,74
External edge	47,08	46,9	3,78	3,6
Gradiente	42,87	43	0,43	0,3

Source: Authors, 2025.

The internal edges, in both polarizations, presented greater disparity in relation to the reference perimeter, reaching almost twice the residue found in the external edge. The gradient presented the best results, reaching residual values below 0.5 (Km²). Even with important differences found in the internal edge, the edges generated by VH still stood out.

The results shown in Table 2 were augmented by a regional-scale accuracy assessment based on regression metrics (Figure 6). The proportion of edge pixels obtained by MM in the VH and VV polarizations was compared to the proportion of cells detected by the reference data, where, as a comparison criterion, the Coefficient of Determination (R^2) is an indication of accuracy, according to Giglio *et al.* (2018). Figure 6 presents a linear regression graph obtained by combining the cells of the reference edges (Y axis) and the reference perimeter obtained through a internal, external and gradient edges (X axis):

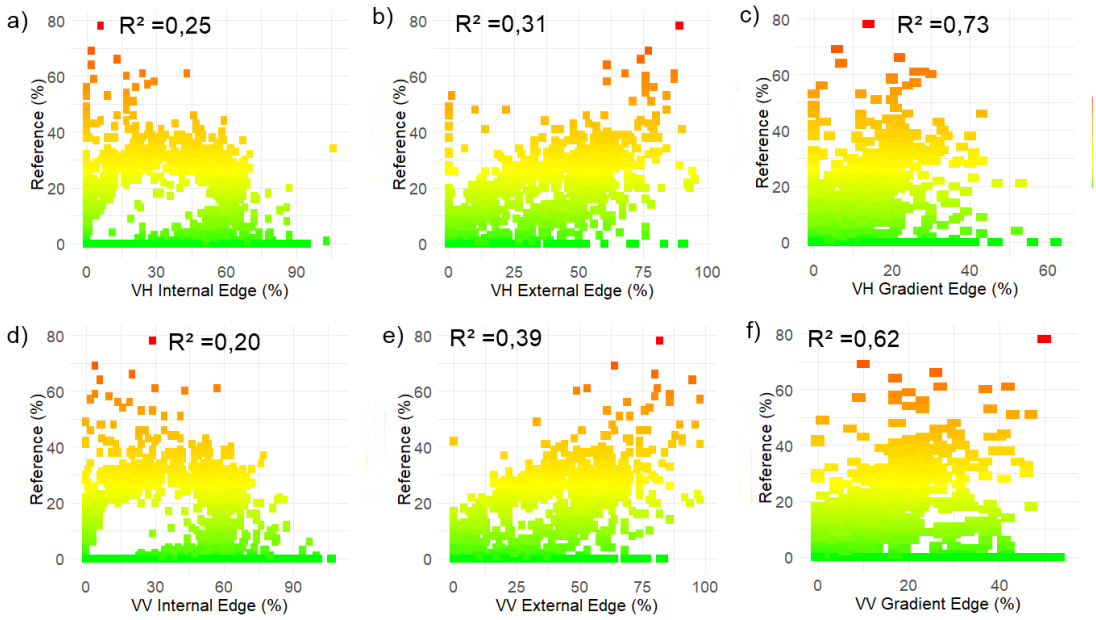

Figure 6. Regression graph obtained by combining all cells of the internal, external and gradient edge.
Figura 6. Gráfico de regressão obtido pela combinação de todas as células da borda interna, externa e do gradiente.

The edges obtained in the VH polarization have a slightly higher precision than the VV, (R^2VH(int): 0,25 vs. R^2VV(int): 0,20), (R^2VH(ext): 0,31 vs. R^2VV(ext): 0,39) and mainly for the gradient edge (R^2VH(grad): 0,73 vs. R^2VV(grad): 0,62) (Figure 6). The Morphological Gradient edges resulted in a better delineation in both polarizations, having as visual pattern thinternal edges, greater coherence with the binarization threshold and the reference data.

DISCUSSION

In this study, the results provided an understanding of the spatiotemporal patterns of land use in a clear-cut polygon in the Amazon, in the State of Mato Grosso - BR, using SAR data and Mathematical Morphology. The objective was, through the edge detection technique, to delineate the forest deforestation edges in one of the most threatened biomes in the world. The edges generated in the VH polarization presented slightly higher precision than the VV polarization, especially for the gradient edges, which was confirmed by the visual analyses in Figures 3, 4, 5 and in the Residue Table (Table 2). Morphological Gradient edges resulted in a more accurate delineation in both polarizations, with thinternal edges and greater coherence with the binarization threshold and reference data. These results reinforce the importance of considering the behavior of radar wave polarizations in the different phases of SAR image processing, since they interact directly with forest dynamics (Bouvet *et al.*, 2018; Ballère *et al.*, 2021), influencing how the signal interacts with trunks, canopy components and degraded areas, directly impacting the products generated.

Studies developed by Fonseca, Tavares and Candeias (2020) show that the automatic extraction of linear features from edge detection techniques emerges as a possibility for use in degraded areas, such as deforestation and forest fires, allowing the interpretation of lineaments and pattern recognition in geophysical data and orbital images. The method aims to transform linear features contained in images or geophysical data into a vector segment automatically, in order to speed up the extraction process and reduce the subjectivity inherent in the manual method. Within this context, according to Silva *et al.* (2021), the state of Mato Grosso, in particular the Amazon/Cerrado transition region, deserves special attention in terms of monitoring the dynamics of land use and coverage, as it constitutes a front of agricultural expansion into the interior of the Brazilian Amazon. Therefore, techniques, such as edge extraction, which allow the extraction of information on land cover automatically, reducing the subjectivity of manual methods, become tools that ensure accuracy, practicality, and expanding the monitoring capacity of deforested areas.

In the target detection process, when the C-band signal reaches the top of the trees, it provides greater sensitivity to the "spatial texture" and structure of the canopy and, consequently, some potential for distinguishing deforestation, that is, they have a greater capacity to detect changes in forest cover for use as an early warning of deforestation (Carreiras *et al.* 2020). This can be seen in Figure 5, where it was possible to observe well-defined edges in sectors of the study area where there was a greater distinction between forests and non-forests. The edge analyses obtained by MM showed that the VV and VH polarizations have similar performance in detecting forest changes. However, the VH polarization obtained the best results and was able to produce edges with less noise distribution. This result can be attributed to the greater sensitivity of VH polarization to volume scattering processes. This sensitivity, in turn, leads to better separation of deforestation classes, compared to VV polarization. Furthermore, in the study by Souza Mendes *et al.* (2019), the authors reported that the best detection of deforestation by SAR image processing methods is related to the direction of the energy pulse, considering that cross-polarizations (VH and HV) provide better discrimination of forest types in the C band, based on the fact that the interaction of microwaves in the plant components is one of the mechanisms that results in the depolarization of incident microwaves. Thus, the different canopy structures generate a wide range of backscattering values, which facilitates the separation of forest and non-forest areas (Hansen; Mitchard; King, 2020).

However, it should be noted that in semi-degraded forests, soil moisture (especially in the C band), planting areas or regions with many active spectral elements in the same area can interfere with detection at different polarizations. This interference is enhanced by changes in the volumetric water content of the soil, which affects the relative dielectric constant, resulting in variations in the backscattering intensity. Furthermore, the structure of leaves and small branches in the upper canopy of mature forests may resemble the dense vegetation of the Amazon biome, leading to similar backscatter responses in the C-band and, consequently, potential interference in image classification processes. Additionally, rough soil conditions and debris remaining after deforestation may also generate intense backscattering, which, despite the high levels of above-ground biomass characteristic of the Amazon biome, may make it difficult to distinguish between different land use classes (Hansen; Mitchard; King, 2020).

CONCLUSIONS

The analyses carried out allow us to conclude that:

- Edge detection based on Mathematical Morphology was effective in preserving spatial details, ensuring the continuity and integrity of the detected edges, despite the grainy texture characteristic of orbital images. However, the results were more satisfactory when applied to images with greater contrast and sharpness, highlighting the importance of these aspects.
- The results confirmed that the applied methods ensure accuracy in segmentation, avoiding problems with the presence of clouds and allowing the detection of different types of forest cover, providing reliable information

about the territory. However, it is important to note that the quality of edge extraction is closely related to the binarization threshold, since radar images, even after the speckle filter, still present texture peaks and noise.

- Although the analysis was local, the method presented in this article allowed the measurement of key elements for monitoring deforestation in the Amazon, generating a cartographic representation of areas susceptible to deforestation at a scale of 1:50,000, based on cartographic visual acuity parameters. However, the best results were obtained when the method was applied to images with greater contrast and sharpness.

REFERENCES

ARÉVALO, P.; OLOFSSON, P.; WOODCOCK, C. E. Continuous monitoring of land change activities and post-disturbance dynamics from Landsat time series: a test methodology for REDD+ reporting. **Remote Sensing of Environment,** Amsterdam, v. 238, p. 111051, mar. 2020. DOI: 10.1016/j.rse.2019.01.013.

BALLÈRE, M.; BOUVET, A.; MERMOZ, S.; TOAN, T. L.; KOLECK, T.; BEDEAU, C.; ANDRÉ, M.; FORESTIER, E.; FRISON, P.; LARDEUX, C. SAR data for tropical forest disturbance alerts in French Guiana: benefit over optical imagery. **Remote Sensing of Environment**, [S.L.], v. 252, p. 112159-112165, jan. 2021. DOI.10.1016/j.rse.2020.112159.

BOUVET, S.; MERMOZ, M.; BALLRE, T.; T. LE TOAN, "Use of the SAR shadowing effect for deforestation detection with Sentinel-1 time series", **Remote Sensing**, [S.L.], v. 10, n. 8, 2018. DOI. 10.3390/rs10081250.

CARREIRAS, J. M. B.; QUEGAN, S.; TANSEY, K.; PAGE, S. Sentinel-1 observation frequency significantly increases burnt area detectability in tropical SE Asia. **Environ. Res. Lett**. [S.L.], v. 15, n. 05 p.4008.2020. DOI. 10.1088/1748-9326/ab7765.

DIAS, L. C. C.; OLIVEIRA-JUNIOR, N. D.; MOTA, J. S.; MONTEIRO, E. C. S.; AMARAL, S.; REGOLIN, A. L.; LUZ, N. B.; SOLER, L.; ALMEIDA, C. A. Assessing dominant production systems in the Eastern Amazon Forest. **Forests**, Basel, v. 16, n. 1, p. 89, 2025.

DRÜKE, M.; THONICKE, K. O fogo pode impedir a recuperação futura da floresta amazônica após o desmatamento em larga escala. **Communications Earth & Environment**, [s.l.], v. 4, p. 248, 2023.

ESA. EUROPEAN SPACE AGENCY. **Sentinel-1 The European Space Agency**. 2021. Disponível em: <https://sentinels.copernicus.eu/web/sentinel/missions/sentinel-1> . Acesso em: 17 abril de 2021.

FONSECA , C, R .; TAVARES JR., R. J.; CANDEIAS, B. L. A. Programação Python e índices físicos na detecção de bordas na Unidade de Conservação Parque Estadual Mata Da Pimenteira (Pernambuco). **Revista Brasileira de Sensoriamento Remoto.** [S.L.], v. 1, n. 2, 2020. ISSN: 2675-5491

GIGLIO, L.; BOSCHETTI, L.; ROY, D. P.; HUMBER, M. L.; JUSTICE, C. O.. The Collection 6 MODIS burned area mapping algorithm and product. **Remote Sensing of Environment**, [S.L.], v. 217, p. 72-85, nov. 2018. DOI.10.1016/j.rse.2018.08.005.

GUISAO-BETANCUR, A.; DÉNIZ, L. G.; MARULANDA-TOBÓN, A. Forest/nonforest segmentation using Sentinel-1 and -2 data fusion in the Bajo Cauca Subregion in Colombia. **Remote Sensing**, Basel, v. 16, n. 1, p. 5, 2023.

HANSEN, J.N.; MITCHARD, E.T.A.; KING, S. Assessing Forest/Non-Forest Separability Using Sentinel-1 C-Band Synthetic Aperture Radar. **Remote Sens**. [S.L.], v.12, p.1899, 2020.

IBGE. Instituto Brasileiro de Geografia e Estatística (2004). **Vegetation Map of Brazil**. Disponível: < ibge.gov.br/en/geosciences/maps/state-maps/19470-brazilianvegetation.html?edicao=22013&t=acesso-ao-produto>

JIN, S.; LIU, Y.; FAGHERAZZI, S.; MI, H.; QIAO, G.; XU, W.; SUN, C.; LIU, Y.; ZHAO, B.; FICHOT, C. G.. River body extraction from sentinel-2A/B MSI images based on an adaptive multi-scale region growth method. **Remote Sensing of Environment**, [S.L.], v. 255, p. 112297, mar. 2021. DOI.10.1016/j.rse.2021.112297.

KAUFMAN, Y.J.; REMER, L. Remote sensing of vegetation in the mid-IR: The 3.75 µm channels. **IEEE Geoscience and Remote Sensi ng Letters**. [S.L.], v 32, p. 672-683, 1994 .

LIBONATI, R.; DACAMARA, C.C; SETZER, A.W.; MORELLI, F.; MELCHIORI, A.E. An Algorithm for Burned Area Detection in the Brazilian Cerrado Using 4 µm MODIS Imagery. **Remote Sensing**, [S.L.], v. 7, p.15782-15803, 2015. DOI. 10.3390/rs71115782

MCGREGOR, I. R.; CONNETTE, G.; GRAY, J. M. A multi-source change detection algorithm supporting user customization and near real-time deforestation detections. **Remote Sensing of Environment**, Amsterdam, v. 308, p. 114195, jul. 2024. DOI: 10.1016/j.rse.2024.114195.

PEREIRA, A. A.; TEIXEIRA, F. R.; LIBONATI, R.; MELCHIORI, E. A.; CARVALHO, L. M. T. Avaliação de índices espectrais para identificação De áreas queimadas no Cerrado utilizando dados Landsat TM. **Revista Brasileira de Cartografia,** [S.L.],v. 68, n. 8, out. 2016.

REICHE, J.; HAMUNYELA, E.; VERBESSELT, J.; HOEKMAN, D.; HEROLD, M. Improving near-real time deforestation monitoring in tropical dry forests by combining dense Sentinel-1 time series with Landsat and ALOS-2 PALSAR-2. **Remote Sensing of Environment**, [S.L.], v. 204, p. 147-161, jan. 2018. DOI.10.1016/j.rse.2017.10.034.

REED, I. S.; YU, X. "Adaptive Multiple-band CFAR Detection of an óptico pattern with unknown distribuição espectral," In: **IEEE Transactions on Acoustics, Speech, and Signal Processing** , 1990, Munique. Anais... IEEE, Munique, v. 38, n. 10, p. 1760-1770, outubro de 1990. DOI. 10.1109 / 29.60107.

SILVA, V. S.; SANO, E. E.; ALMEIDA, T. DE; MESQUITA JÚNIOR, H. N. DE. Discriminação de Classes de Cobertura Vegetal em uma Região de Transição Amazônia/Cerrado no Estado de Mato Grosso por meio de Imagens do Satélite ALOS-2/PALSAR-2. **Revista Brasileira de Cartografia**, [S.L.], v. 73, n. 1, p. 1-16, 18 fev. 2021.DOI. 10.14393/rbcv73n1-48516.

SILVA JUNIOR, Celso H. L.; PESSÔA, Ana C. M.; CARVALHO, Nathália S.; REIS, João B. C.; ANDERSON, Liana O.; ARAGÃO, Luiz E. O. C.. The Brazilian Amazon deforestation rate in 2020 is the greatest of the decade. **Nature Ecology & Evolution**, [S.L.], v. 5, n. 2, p. 144-145, 21 dez. 2020. Springer Science and Business Media LLC. http://dx.doi.org/10.1038/s41559-020-01368-x

SLAGTER, B.; FESENMYER, K.; HETHCOAT, M.; BELAIR, E.; ELLIS, P.; KLEINSCHROTH, F.; PEÑA-CLAROS, M.; HEROLD, M.; REICHE, J. Monitoring road development in Congo Basin forests with multi-sensor satellite imagery and deep learning. **Remote Sensing of Environment**, Amsterdam, v. 315, p. 114380, dez. 2024. DOI: 10.1016/j.rse.2024.114380.

SOUZA MENDES, F.; BARON, D.; GEROLD, G.; LIESENBERG, V.; ERASMI, S. Optical and SAR Remote Sensing Synergism for Mapping Vegetation Types in the Endangered Cerrado/Amazon Ecotone of Nova Mutum—Mato Grosso. **Remote Sensing**. [S.L.], v. 11, n. 10, p. 1161-1171, maio 2019. DOI. 10.3390/rs11101161.

YANG, H.; SONG, M.; SON, H.; KIM, R.; CHOI, E. Evaluating REDD+ readiness: high-potential countries based on MRV capacity. **Forests**, Basel, v. 16, n. 1, p. 67, 2025.

ZHANG, Y.; LING, F.; WANG, X.; FOODY, G. M.; BOYD, D. S.; LI, X.; DU, Y.; ATKINSON, P. M. Tracking small-scale tropical forest disturbances: fusing the Landsat and Sentinel-2 data record. **Remote Sensing of Environment**, Amsterdam, v. 261, p. 112470, ago. 2021.